Effect of miR-21-3p on lung injury in rats with traumatic hemorrhagic shock resuscitated with sodium bicarbonate Ringer's solution

Shugen Xu[1,2,3], Zhaolei Qiu[4,5], Chuanming Zheng[4,5], Lei Li[4,5], Hai Jiang[4,5], Fulong Zhang[4,5], Zhenjie Wang[1,2,4,5]

[1]Cheeloo College of Medicine, Shandong University, Jinan, China; [2]Division of Life Sciences and Medicine, The First Affiliated Hospital of USTC, University of Science and Technology of China, Hefei, China; [3]Department of Emergency Medicine, The Affiliated Changsha Central Hospital, Hengyang Medical School, University of South China, Changsha, China; [4]Department of Emergency Medicine, The First Affiliated Hospital of Bengbu Medical College, Bengbu, China; [5]Institute of Emergency and Critical Care Medicine, The First Affiliated Hospital of Bengbu Medical College, Bengbu, China

Contributions: (I) Conception and design: Z Wang, S Xu; (II) Administrative support: Z Wang; (III) Provision of study materials or patients: S Xu; (IV) Collection and assembly of data: S Xu, Z Qiu, C Zheng, L Li, H Jiang, F Zhang; (V) Data analysis and interpretation: S Xu; (VI) Manuscript writing: All authors; (VII) Final approval of manuscript: All authors.

Correspondence to: Zhenjie Wang. Cheeloo College of Medicine, Shandong University, 27 Shandan Road, Jinan 250100, China.
Email: ahbyfywzj@163.com.

Background: Restricted fluid resuscitation is the most important early method for treating traumatic hemorrhagic shock (THS). This study sought to explore whether micro ribonucleic acid (miR)-21-3p affected resuscitated THS rats by regulating the glycocalyx and inflammation.

Methods: MiRNAs extracted from the lung tissues were analyzed by miRNA microarray assays. A rat model of THS was induced by hemorrhage from a left femur fracture. The pathological change in the lung tissues and glycocalyx structure was observed by hematoxylin and eosin staining and a transmission electron microscope examination. The miR-21-3p expression in the lung tissues and serum was detected by real-time quantitative polymerase chain reaction (RT-qPCR). The levels of glycocalyx-related factors and inflammation-related factors were determined by enzyme linked immunosorbent assays. The expression of glycocalyx-related proteins, cell junction-related proteins, and the phosphatidylinositol 3-kinase (PI3K)/protein kinase B (Akt)/nuclear factor kappa B (NF-κB) signaling pathway-related proteins was analyzed by Western blot.

Results: After RT-qPCR verification, the variation trend of miR-21-3p was in line with expected trends. The mean arterial pressure (MAP) and heart rate (HR) were decreased, and the lung injury and damage to the glycocalyx were all aggravated in the THS rats resuscitated with sodium bicarbonate Ringer's solution (BRS) or sodium lactate Ringer's solution (LRS). The expression of miR-21-3p was decreased in the THS rats resuscitated with BRS and increased in the THS rats resuscitated with LRS, and the upregulation of miR-21-3p further decreased the MAP and HR, and increased the levels of syndecan-1 (SDC-1), heparanase-1 (HPA1), interleukin (IL)-6, IL-1β, and tumor necrosis factor alpha (TNF-α) in the serum of the THS rats resuscitated with BRS. The upregulation of miR-21-3p also increased the expression of SDC-1, HPA1, β-catenin, matrix metallopeptidase (MMP)2, and MMP9, but decreased the expression of E-cadherin (E-cad) and activated the PI3K/Akt/NF-κB signaling pathway in the THS rats resuscitated with BRS and transfected with miR-21-3p compared to that of the THS rats resuscitated with BRS and transfected with miR-negative control (NC).

Conclusions: miR-21-3p promoted inflammation and glycocalyx damage by activating the PI3K/Akt/NF-κB signaling pathway, thereby aggravating the lung injury in the THS rats resuscitated with BRS.

Keywords: MiR-21-3p; lung injury; traumatic hemorrhagic shock (THS); sodium bicarbonate Ringer's solution (BRS)

Submitted Sep 23, 2022. Accepted for publication Nov 18, 2022.
doi: 10.21037/atm-22-5148
View this article at: https://dx.doi.org/10.21037/atm-22-5148

Introduction

Traumatic and hemorrhagic shock (THS) can lead to systemic inflammatory response syndrome and multiple organ dysfunction syndrome, and ultimately multiple organ failure and death (1). In recent years, the mortality rate of THS has decreased, but the incidence rate has continued to rise (2), and about 1.9 million patients die from hemorrhagic shock every year (3). Interventions contributed to bleeding control and hemostatic resuscitation have advantages on decreasing the mortality of hemorrhagic injury. Applying these novel strategies to the casualty prehospital phase of care, particularly in tactical or austere environments, may be beneficial for hemorrhage mitigation to extend the window of survival to definitive care (4). The incidence of lung injury after THS is approximately 40%. Lung injury may develop into acute respiratory distress syndrome (ARDS) and is one of the main causes of death of THS (4). Lung injury after THS is characterized by an excessive uncontrolled inflammatory response and vascular endothelial injury (5-7). Thus, the reduction of the pulmonary inflammatory response and vascular endothelial injury are important in improving the curative effect of THS.

Restricted fluid resuscitation is the most important early treatment for THS patients and can improve patients' recovery from THS (8,9). Effective fluid resuscitation not only improves the tissue perfusion of patients and microcirculation oxygen delivery (10), but also inhibits inflammation (11). Currently, the liquids commonly used for clinical liquid resuscitation include sodium lactate Ringer's solution (LRS) and acetic Ringer's solution (12). Recent studies suggested that sodium BRS, a novel resuscitate crystal-fluid, had obvious advantages over conventional fluids in the treatment of THS (13,14). Previous studies indicated that BRS could directly participate in acid-base metabolism, amend base excess values, keep acid-base balance, decline lactate levels, and suppress lung cell apoptosis (15-18). Early resuscitation of patients with THS with BRS can better inhibit the expression of inflammatory factors in peripheral blood and reduce the blood lactate value, which has more advantages than that of LRS (13).

The glycocalyx is a polysaccharide structure inside the lumen of endothelial cells, and an intact glycocalyx is very important for maintaining vascular homeostasis. Glycocalyx shedding may lead to vascular permeability and increase coagulation system activation and leukocyte adhesion (19,20). In the inflammatory cascade, the structure and function of the glycocalyx in vascular endothelial cells were changed and glycocalyx also participated in the regulation of the occurrence and development of inflammation. A previous study reported that vascular endothelial dysfunction and increased vascular permeability were closely related to mortality in THS patients (21). A study of a model of hemorrhagic shock in dogs showed that glycocalyx injury was affected by inflammatory factors (22). Zhang *et al.* (23) hypothesized that there was a vicious cycle between a damaged endovascular glycocalyx and endothelial cell dysfunction.

Micro ribonucleic acids (miRNAs) are small and non-coding RNAs, 19–24 nucleotides in length, that can bind with the 3'untranslated region of a messenger RNA (mRNA)

Highlight box

Key findings

- miR-21-3p promoted inflammation and glycocalyx damage by activating the PI3K/Akt/NF-κB signaling pathway, thereby aggravating the lung injury in the THS rats resuscitated with BRS.

What is known and what is new?

- miR-21-3p expression was increased in the brain after traumatic brain injury (TBI) and human vascular endothelial cells induced by high glucose. miR-21-3p knockdown could alleviate blood-brain barrier damage leakage after TBI and improve atherosclerotic lesions in diabetic atherosclerotic mice;
- miR-21-3p expression was increased in THS rats and aggravated the lung injury in the THS rats resuscitated with BRS through destroying the endodermis glycocalyx in the lung.

What is the implication, and what should change now?

- miR-21-3p may be a potential target for the treatment of THS.

sequence to regulate the expression of its target genes (24). Ge *et al.* found that miR-21-3p expression was increased in the brain after traumatic brain injury (TBI), and miR-21-3p inhibition decreased blood-brain barrier damage leakage after TBI by suppressing apoptosis and the inflammation of brain microvascular endothelial cells (25). MiR-21-3p expression was found to be decreased by human umbilical vein endothelial cell (HUVEC)-derived exosomes and miR-21-3p downregulation could suppress the apoptosis of the hypoxia/reoxygenation-treated neural cells (26). MiR-21-3p expression was also found to be upregulated in human vascular endothelial cells induced by high glucose, and miR-21-3p knockdown was found to improve atherosclerotic lesions in diabetic atherosclerotic mice by reducing the infiltration of inflammatory cells (27). However, to date, no study has examined the role of miR-21-3p in THS. Thus, this study sought to whether miR-21-3p affected resuscitated THS rats by regulating the glycocalyx and inflammation, and the underlying mechanism. We present the following article in accordance with the ARRIVE reporting checklist (available at https://atm.amegroups.com/article/view/10.21037/atm-22-5148/rc).

Methods

Animals

A total of 36 male Sprague-Dawley rats [specific-pathogen free (SPF) grade, 8–10 weeks old, weighing 220–250 g] were purchased from Shanghai Jiesijie Experimental Animal Co. Ltd. and maintained in an environmentally controlled room (22±2 ℃, 12-h light-dark cycle) with free access to standard animal feed and filtered tap water for 7 days to acclimatize to their new environment. Animal experiments were performed under a project license (No. 2022101) granted by the Animal Care and Use Committee and the Animal Ethics Committee of The First Affiliated Hospital of Bengbu Medical College, in compliance with national guidelines for the care and use of animals. A protocol was prepared before the study without registration.

Preparation of the lentivirus vector

The lentiviral vector (OBIO, Shanghai, China) was encoded with rno-miR-21-3p for the upregulation of miR-21-3p. A blank lentiviral vector was employed as the negative control (miR-NC).

Animal grouping

The rats (n=36) were randomly divided into the following 6 groups: (I) the sham group (n=6) rats, which underwent the same anesthetic and surgical procedures, but on which neither trauma/hemorrhage nor fluid resuscitation was performed; (II) the model group (n=6) rats, which underwent the trauma/hemorrhage procedures, but which did not undergo fluid resuscitation; (III) the BRS group (n=6) rats, which underwent the trauma/hemorrhage procedures and resuscitation with BRS; (IV) the LRS group (n=6) rats, which underwent the trauma/hemorrhage procedures and resuscitation with LRS; (V) the BRS + miR-21-3p group (n=6) rats, which were injected with lentivirus-mediated miR-21-3p via the tail vein 72 h before modeling, and then underwent the same procedures as those performed in the BRS group; (VI) the BRS + miR-NC group (n=6) rats, which were injected with blank lentiviral vector via the tail vein 72 h before modeling, and then underwent the same procedures as those performed in the BRS group.

Establishment of rats with THS

The rats were anesthetized intraperitoneally with sodium pentobarbital (40 mg/kg body weight) and were allowed to waken. Under aseptic conditions, the left femur mid-diaphyseal transverse fracture was made, and a hemorrhage was induced via a right femoral artery catheter until the mean arterial pressure (MAP) decreased to 35±5 mmHg, which was maintained for 1 h. The right femoral vein was used for fluid resuscitation, and the left femoral artery was catheterized to measure MAP. Afterwards, the rats were resuscitated with 2 times the shed blood volume in the form of BRS or LRS for a period of 20 min at a constant rate (20 mL/h) to manage the shock. Finally, the catheters were removed, the vessels were ligated, and the incisions were closed. The MAP and heart rate (HR) were recorded at the end of resuscitation (0 h) and 3 h post-resuscitation. When the experiment was finished, blood was collected from all rats for analysis at 3 h post-resuscitation, and the lung tissues were resected at 3 h post-resuscitation when the rats were anesthetized by the intraperitoneal injection of pentobarbital sodium (50 mg/kg body weight). The adverse event in experiment was the organ injury. When the experiment was finished, all rats were to be euthanized with 1% pentobarbital sodium (150 mg/kg; i.p.).

MiRNA microarray analysis

A microarray analysis of the miRNAs of the lung tissues was performed using the samples from the BRS and model groups of rats (n=6) on Illumina sequencing platforms. Differentially expressed miRNAs between the two groups were identified based on the fold-change and P values.

Hematoxylin and eosin staining and transmission electron microscope examination

The lung tissues of the rats were fixed with 4% paraformaldehyde buffer and embedded into paraffin, and then cut into 5-μm slices. After processing with xylene, gradient ethanol, and distilled water in turn, the tissue slices were stained with hematoxylin (Beyotime, China) for 10 min at room temperature. Next, the slices were treated with ethanolamine hydrochloride solution for 20 s and washed with distilled water for 5 min. Subsequently, the tissue slices were dyed with eosin (Beyotime) for 3 min at room temperature. After being transparentized with xylene and sealed with neutral gel, the tissue slices were observed under a light microscope (Olypums).

The lung tissues of the rats were fixed in 0.1 mol/L of sodium cacodylate solution (2.5% glutaraldehyde and 2% lanthanum nitrate hydrate) at 4 ℃ for 24 h. The fixed specimens were rinsed with 0.1 mol/L of sodium cacodylate buffer, and then fixed with 1% osmium tetroxide for 1.5 h. After being rinsed with buffer, the specimens were dehydrated by gradient, and immersed and embedded by Epon812. Ultrathin sections with a thickness of 60 nm were taken, observed and photographed directly under a transmission electron microscope.

RT-qPCR

Total miRNA was extracted from serum and lung tissues using Trizol® reagent (Invitrogen; Thermo Fisher Scientific, Inc.). Next, complementary deoxyribonucleic acid was synthesized from the mRNA using the PrimeScript RT Reagent kit (Takara, Japan). Subsequently, Synergy Brands (SYBR) premix Ex Taq™ II polymerase chain reaction (PCR) kit (Takara) was used to perform the amplification on an ABI 7500 quantitative PCR (qPCR) instrument (ABI/Perkin Elmer). The relative miRNA expressions were calculated using the $2^{-\Delta\Delta Ct}$ method and then were normalized to U6 (28).

ELISAs

The levels of syndecan-1 (SDC-1), heparanase-1 (HPA1), interleukin (IL)-6, IL-1β, and tumor necrosis factor alpha (TNF-α) in the serum of the rats were detected by rat enzyme linked immunosorbent assay (ELISA) kits of SDC-1 (ml037982; Enzyme-linked Biotechnology, China), HPA1 (JL21427; Jianglai Biotechnology, China), IL-6 (ml102828; Enzyme-linked Biotechnology), IL-1β (ml003057; Enzyme-linked Biotechnology), and TNF-α (ml002859; Enzyme-linked Biotechnology). In brief, serum (50 μL) and standard samples (50 μL) were added into the 96-well plate of each ELISA kit, followed by 100 μL of horseradish peroxidase (HRP)-marked antibody, and then incubated at 37 ℃ for 1 h. After the 96-well plate was washed by 300 μL of wash buffer for 1 min, substrate A (50 μL) and substrate B (50 μL) were respectively added to the 96-well plate, which was then incubated at 37 ℃ for 15 min avoiding light. After 50 μL of stop buffer was added to the 96-well plate, the reaction was terminated, and the absorbance was measured under 450 nm using the IMARK microplate reader (Bio-Rad, USA).

Western blot

The total protein in the lung tissues of the rats was extracted by radioimmunoprecipitation assay buffer, and protein centration was determined by a bicinchoninic acid (BCA) detection kit. After the denaturation, 30 μg of protein was electrophoresed to sodium dodecyl sulfate-polyacrylamide gel electrophoresis gel, and then transferred onto the polyvinylidene fluoride (PVDF) membranes. After being blocked with 5% non-fat milk for 1 h at room temperature, the PVDF membranes were further incubated with the following primary antibodies at 4 ℃ overnight: SDC-1 (bs-1309R; dilution, 1:1,000; Bioss, China), HPA1 (bs-1541R; dilution, 1:1,000; Bioss), E-cadherin (E-cad) (bs-10009R; dilution, 1:1,000; Bioss), β-catenin (bs-1165R; dilution, 1:1,000; Bioss), matrix metallopeptidase (MMP)2 (bs-0412R; dilution, 1:1,000; Bioss), MMP9 (bs-4593R; dilution, 1:1,000; Bioss), phosphatidylinositol 3-kinase (PI3K) (bs-10657R; dilution, 1:1,000; Bioss), p-PI3K (bs-6417R; dilution, 1:1,000; Bioss), protein kinase B (Akt) (bs-0115R; dilution, 1:1,000; Bioss), p-Akt (bs-0876R; dilution, 1:1,000; Bioss), P65 (bs-0465R; dilution, 1:1,000; Bioss), p-P65 (S536) (bs-0982R; dilution, 1:1,000; Bioss), acetylated (ac)-P65 (Lys310) (bs-23216R; dilution, 1:1,000; Bioss), and glyceraldehyde 3-phosphate dehydrogenase

(GAPDH) (bs-2188R; dilution, 1:2,000; Bioss). The next day, the membranes were incubated with anti-rabbit immunoglobulin G (bs-80295G-HRP; dilution, 1:5,000; Bioss) at room temperature for 2 h. The protein bands were examined by an enhanced chemiluminescence kit, and ImageJ 1.8.0 software (national institutes of Health) was used to analyze the bands intensity.

Statistical analysis

The data are represented as the mean ± standard deviation (SD) of at least three independent experiments, and were statistically analyzed by GraphPad Prism 8.0 (GraphPad Software). The data were compared among groups by an analysis of variance. Tukey's test was applied as the *post-hoc* test. A P-value <0.05 was considered to be statistically different.

Results

MiR-21-3p was chosen as the differentially expressed gene in the THS rats after different treatments

MiRNA microarray assays of the lung tissues of rats in the sham, model, BRS, and LRS groups revealed that a total of 10 miRNAs were differentially expressed in the lung tissue of the THS rats. The 10 differentially expressed miRNAs identified by the sequencing analysis were verified by real-time-qPCR (RT-qPCR) (*Figure 1*), and the variation trend of miR-21-3p was in line with expected trends. Thus, miR-21-3p was chosen for the subsequent experiment.

MiR-21-3p decreased the MAP and HR of the BRS-treated THS rats

At the end of liquid resuscitation (0 h), the MAP (*Figure 2A*) and HR (*Figure 2B*) of the rats in the model group were very low, and the survival state of the rats was poor. Both the MAP and HR recovered significantly after fluid infusion, and the MAP and HR of the rats in the BRS group were better than those of the rats in the LRS group. After the miR-21-3p intervention, the MAP and HR of the rats decreased significantly compared to those in the BRS group, indicating that miR-21-3p was an effective factor affecting injury induced by THS. Notably, 3 h after the fluid resuscitation was finished, the MAP and HR of the rats in the model group were still very low but the MAP and HR of the rats in the remaining groups had recovered and remained at a similar level.

MiR-21-3p caused damage to the glycocalyx and lung tissues of the BRS-treated THS rats

As *Figure 3* shows, compared to the sham group, the lung tissues of the model group showed obvious edema, alveolar wall thickening, tissue bleeding, and inflammatory cell infiltration. In the BRS group, injury was aggravated, edema and alveolar wall thickening were aggravated, and a small amount of bleeding was observed in the tissues. The LRS group showed more severe lung edema and more inflammatory cell infiltration than the BRS group. Compared to the BRS + miR-NC group, the degree of lung tissue edema and alveolar wall thickening were significantly increased, and obvious bleeding was observed in the tissues of the BRS + miR-21-3p group. Alveolar wall thickening and inflammatory cell infiltration were observed in the BRS + miR-NC group, and the degree of damage was similar to that of the BRS group. As *Figure 4* shows, in the sham group, the glycocalyx of the lung tissue remained intact. Conversely, the glycocalyx in the model group was broken and disorganized. The glycocalyx of the BRS and LRS groups were serious and irregular, among which the glycocalyx of the LRS group was thinner and less lanthanum nitrate was deposited. The glycocalyx was significantly thinner and the deposition of lanthanum nitrate was significantly reduced in the BRS + miR-21-3p group compared to the BRS + miR-NC group. Thus, the damage of the LRS group was more serious than that of BRS group, and the damage of the BRS + miR-21-3p group was more serious than that of the BRS + miR-NC group.

MiR-21-3p expression was decreased in the lung tissues and serum of the THS rats treated with BRS

In the lung tissues (*Figure 5A*) and serum (*Figure 5B*) of the rats, compared to the sham group, the expression level of miR-21-3p of the model group was significantly increased, that of the BRS group was lower and that of the LRS group was higher than that of the model group. The expression level of miR-21-3 of the BRS + miR-21-3p group was significantly increased compared to that of the BRS group.

MiR-21-3p destroyed the glycocalyx and induced inflammation in the THS rats treated with BRS

The expression levels of glycocalyx-related proteins

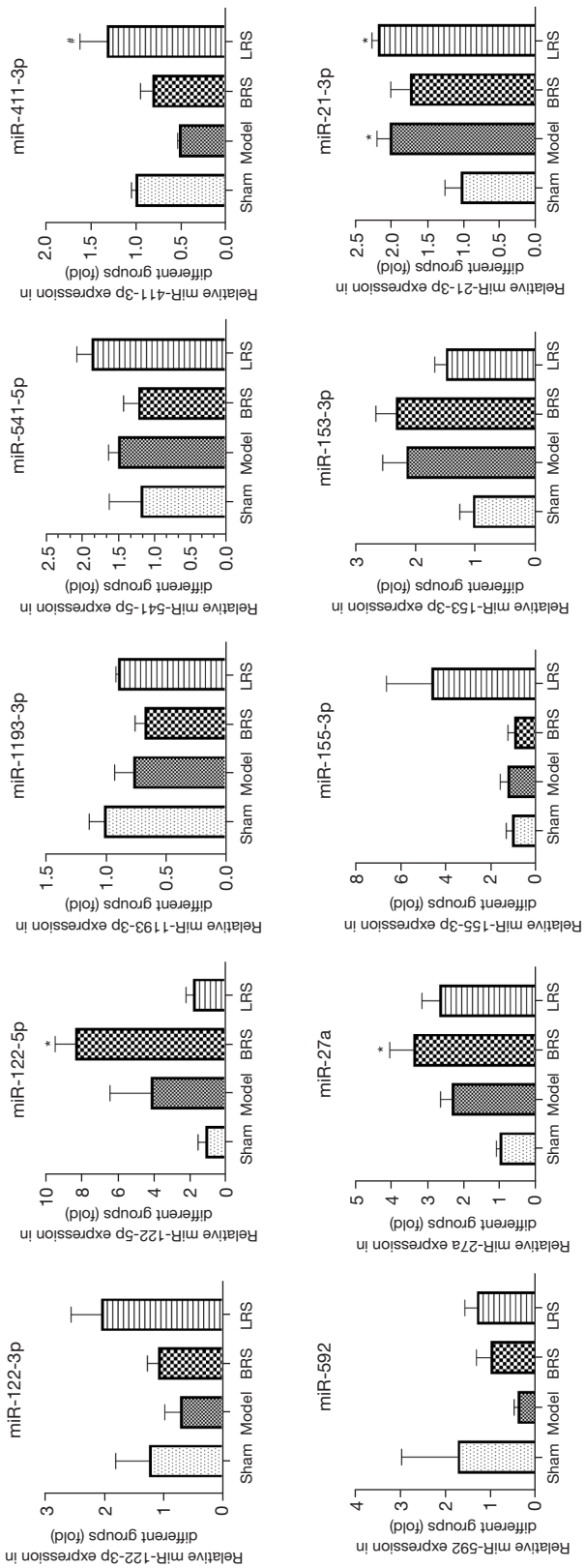

Figure 1 MiR-21-3p was chosen as the differentially expressed gene of the THS rats after different treatments. The expression of 10 differentially expressed miRNAs in the lung tissue of the THS rats receiving BRS or LRS were verified by RT-qPCR. *, $P<0.05$ *vs.* sham; #, $P<0.05$ *vs.* model. THS, traumatic hemorrhagic shock; BRS, bicarbonate Ringer's solution; LRS, lactate Ringer's solution; RT-qPCR, real-time quantitative polymerase chain reaction.

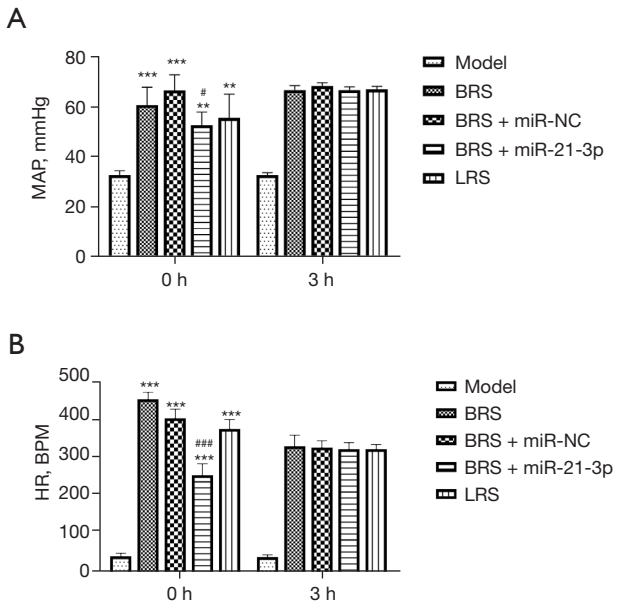

Figure 2 MiR-21-3p decreased the MAP and HR of the BRS-treated THS rats. (A) MAP; (B) HR. **, P<0.01; ***, P<0.001, *vs.* model. #, P<0.05; ###, P<0.001, *vs.* BRS + miR-NC. MAP, mean arterial pressure; HR, heart rate; BRS, bicarbonate Ringer's solution; LRS, lactate Ringer's solution; THS, traumatic hemorrhagic shock; NC, negative control; BPM, beats per minute.

(i.e., SDC-1 and HPA1) (*Figure 6A*), and inflammation-related proteins (i.e., IL-6, IL-1β, and TNF-α) (*Figure 6B*) were significantly increased in the model group. The expression levels of SDC-1 and IL-6 in the BRS group and the expression levels of SDC-1, HPA1, IL-6, IL-1β, and TNF-α in the LRS group were higher than those in the model group. Compared to the BRS + miR-NC group, the expression levels of the above-mentioned proteins were all significantly increased in the BRS + miR-21-3p group.

MiR-21-3p regulated the PI3K/Akt/NF-κB signaling pathway

As *Figure* 7 shows, the expression of SDC-1, HPA1, β-catenin, MMP2, and MMP9 was upregulated in the model group, and was further increased in the BRS or LRS group, while E-cad expression was decreased in the model group, and further downregulated in the BRS and LRS groups. The expression of p-PI3K, p-Akt, p-p65, and ac-p65 was increased in the model group, and was promoted by BRS or LRS. Except for E-cad expression, the expression of all the other proteins was increased in the BRS + miR-21-3p group compared to the BRS + miR-NC group. E-cad expression was decreased in the BRS + miR-21-3p group compared to the BRS + miR-NC group.

Discussion

The pathogenesis of acute lung injury (ALI)/ARDS after THS is complex. Various mechanisms, such as uncontrolled inflammatory response, abnormal coagulation and fibrinolysis, oxidative stress imbalance and endothelial function destruction, are involved in the occurrence and development of ALI. The inflammatory response in the lung is out of control after THS. Lung ischemia-reperfusion injury and apoptosis are the main mechanisms of ALI/ARDS in THS. The damage of the gastrointestinal mucosal barrier caused by intestinal ischemia, the translocation of bacteria and endotoxin into the blood caused by enterogenic bacteremia and endotoxemia are the important factors of ALI/ARDS after THS (29).

THS initiates a systemic inflammatory response, activates inflammatory cells to release a series of bioactive pro-inflammatory factors (TNF-α, IL-6, and IL-8), which in turn leads to obvious inflammatory responses and even inflammatory storms, and inflammation may persist after fluid resuscitation (30,31). Relevant animal research has shown that the injection of LRS promotes the oxidative stress response of neutrophils, which in turn promotes the expression of IL-6, TNF-α, and other cytokines (32). Research showed that the level of IL-6 in patients with ALI was significantly increased, which activated neutrophils and caused them to accumulate in the inflammatory site of injury, and created alveolar capillary endothelial cells and alveolar epithelial cells injury, leading to the occurrence of ARDS (33). In this study, the levels of IL-6, IL-1β, and TNF-α increased continuously in the LRS group compared to the model group. Additionally, the level of IL-6 in the BRS group was higher than that in the model group, but there was no statistically significant difference in the IL-1β and TNF-α levels between the BRS and model groups.

The glycocalyx of vascular endothelial cells is closely related to inflammation, which degrades and decreases the inflammatory response, and is related to the adhesion of white blood cells and changes in vascular permeability (34). The glycocalyx also serves as a blood vessel protector, providing a buffer for the cell membrane, preventing it from chemical damage, and maintaining the normal physiological function of endothelial cells (35). In a shock cell model, hypoxia was shown to damage the glycocalyx,

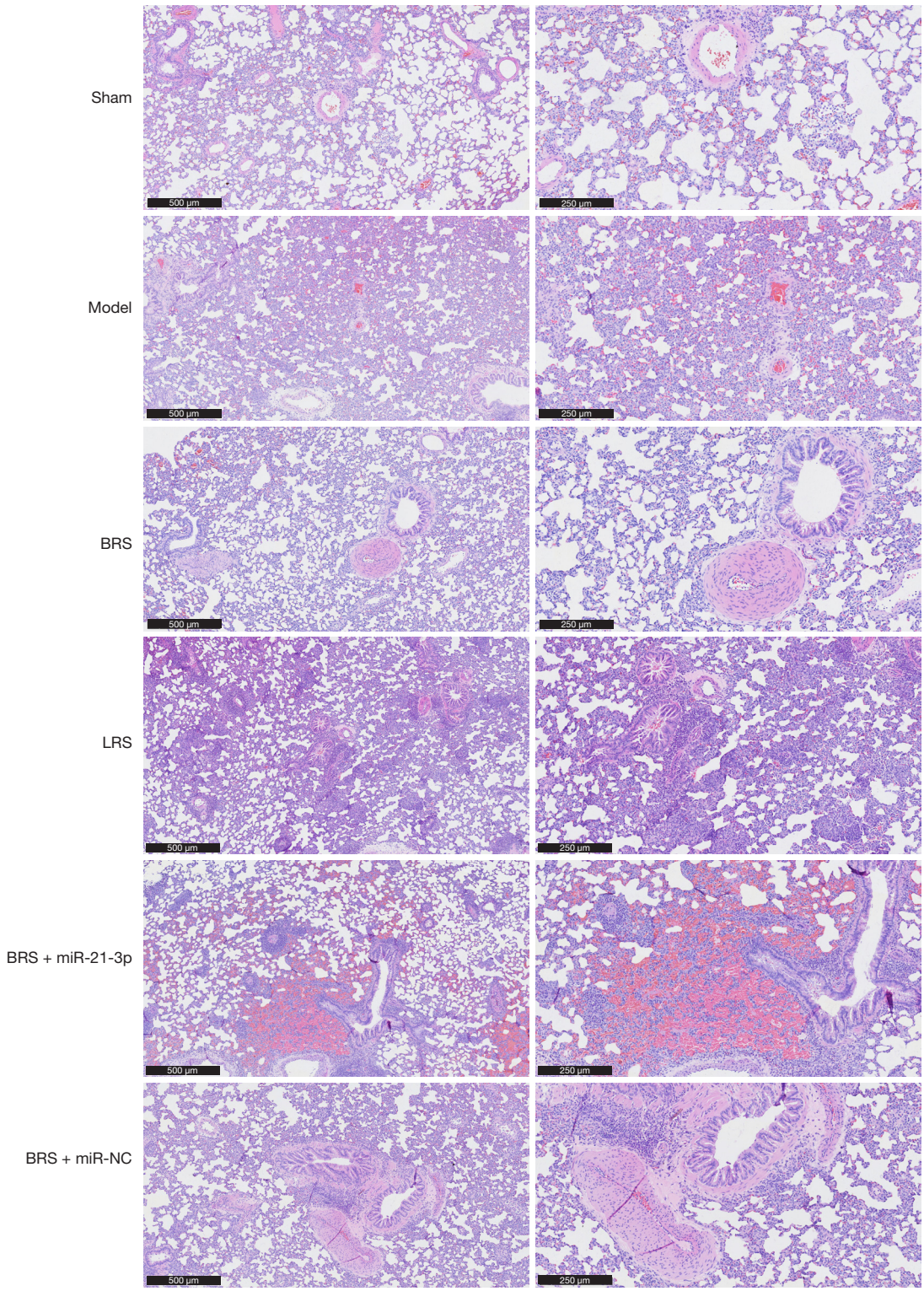

Figure 3 MiR-21-3p caused damage to the lung tissues of the BRS-treated THS rats. A pathological change in the lung tissues of the BRS-treated THS rats transfected with lentivirus-mediated miR-21-3p was observed by hematoxylin and eosin staining. THS, traumatic hemorrhagic shock; BRS, bicarbonate Ringer's solution; LRS, lactate Ringer's solution; NC, negative control.

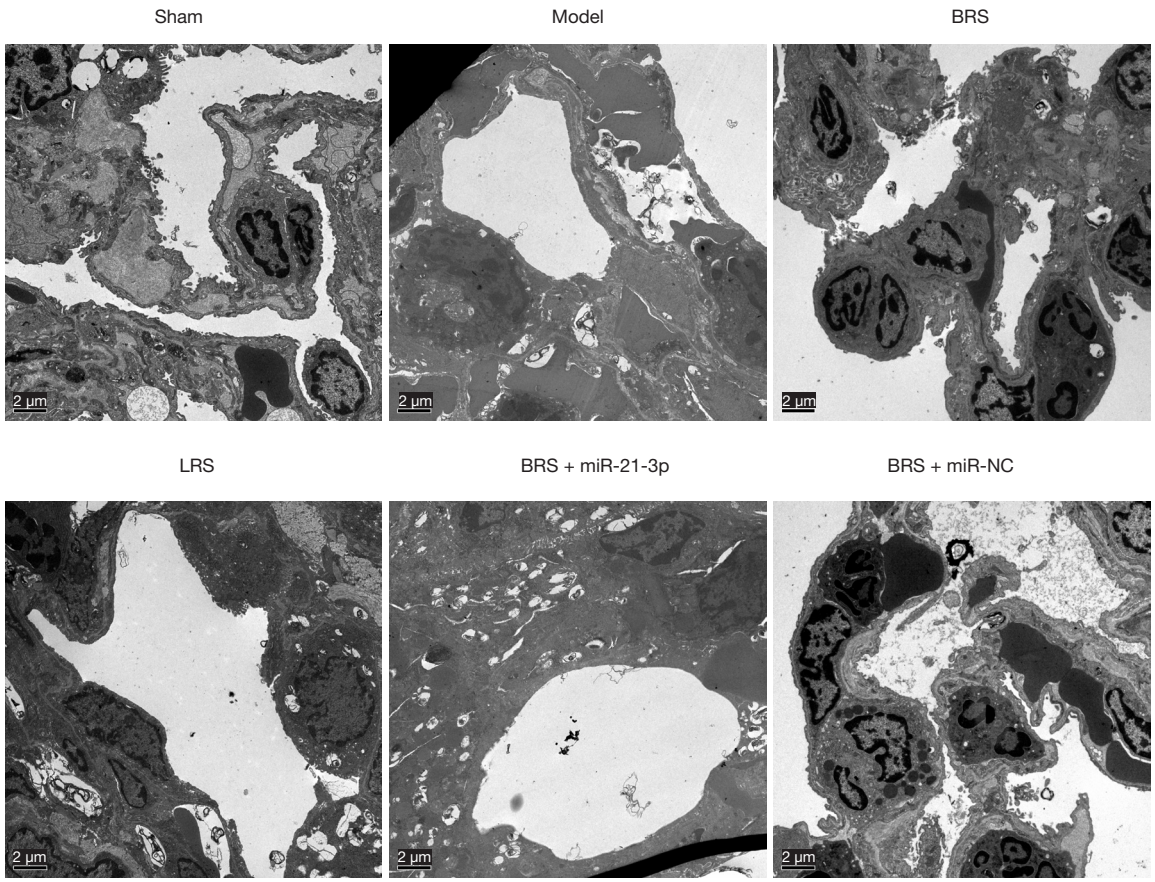

Figure 4 MiR-21-3p caused damage to the glycocalyx of the BRS-treated THS rats. The glycocalyx structure of pulmonary vascular endothelial cells in the BRS-treated THS rats transfected with lentivirus-mediated miR-21-3p was observed by transmission electron microscope examination. THS, traumatic hemorrhagic shock; BRS, bicarbonate Ringer's solution; LRS, lactate Ringer's solution; NC, negative control.

and hypoxia/reoxygenation was shown to cause greater damage to the glycocalyx compared to normal cells (36). This study showed that the glycocalyx was destroyed in the model group, which was further damaged by BRS and LRS treatment. Wiesinger (37) observed cultured pulmonary vascular endothelial cells and found that both lipopolysaccharide (LPS) and TNF-α rapidly reduced the hardness and thickness of the glycocalyx, broke the continuity of the glycocalyx and mediated the damage to the glycocalyx. We found that LRS induced a stronger inflammatory response than BRS; thus, the LRS group had thinner glycocalyx and less lanthanum nitrate depositions than the BRS groups.

HPA1 and MMP9 are destructive factors of the glycocalyx, and heparin sulfate (HS) and SDC-1 are the markers of glycocalyx abscission. HPA1 is an enzyme that decompresses HS, and MMP9 can degrade SDC-1 (38,39). After hemorrhagic shock, a large number of inflammatory factors are produced in the body, which can directly destroy the adhesion and reduce the expression of adhesion molecules, thereby reducing the function of cell adhesion (40,41). Studies have shown that MMPs overexpressed in pathological conditions can directly destroy the components of endodermis glycocalyx, resulting in the destruction of the structure and function of the endodermis glycocalyx. For example, Bauer *et al.* and Higashida *et al.* found that the level of MMP2/MMP9 in the MMP family increased significantly in cerebral ischemia and other pathological conditions (42,43). Additionally, MMP2 and MMP9 can directly affect the molecular structure of chondroitin sulfate in endodermis glycocalyx, causing the abnormal structure of the endodermis glycocalyx, and finally causing the

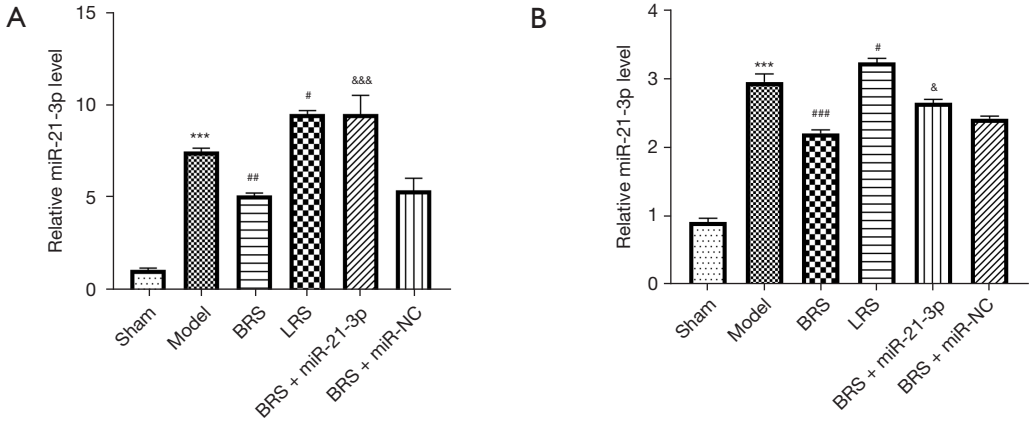

Figure 5 MiR-21-3p expression was increased in the lung tissues and serum of the THS rats treated with BRS. The expression of miR-21-3p in the lung tissues (A) and serum (B) of the THS rats treated with BRS was detected by RT-qPCR. ***, P<0.001, *vs.* sham. #, P<0.05; ##, P<0.01; ###, P<0.001, *vs.* model. &, P<0.05; &&&, P<0.001, *vs.* BRS + miR-NC. THS, traumatic hemorrhagic shock; BRS, bicarbonate Ringer's solution; LRS, lactate Ringer's solution; NC, negative control; RT-qPCR, real-time quantitative polymerase chain reaction.

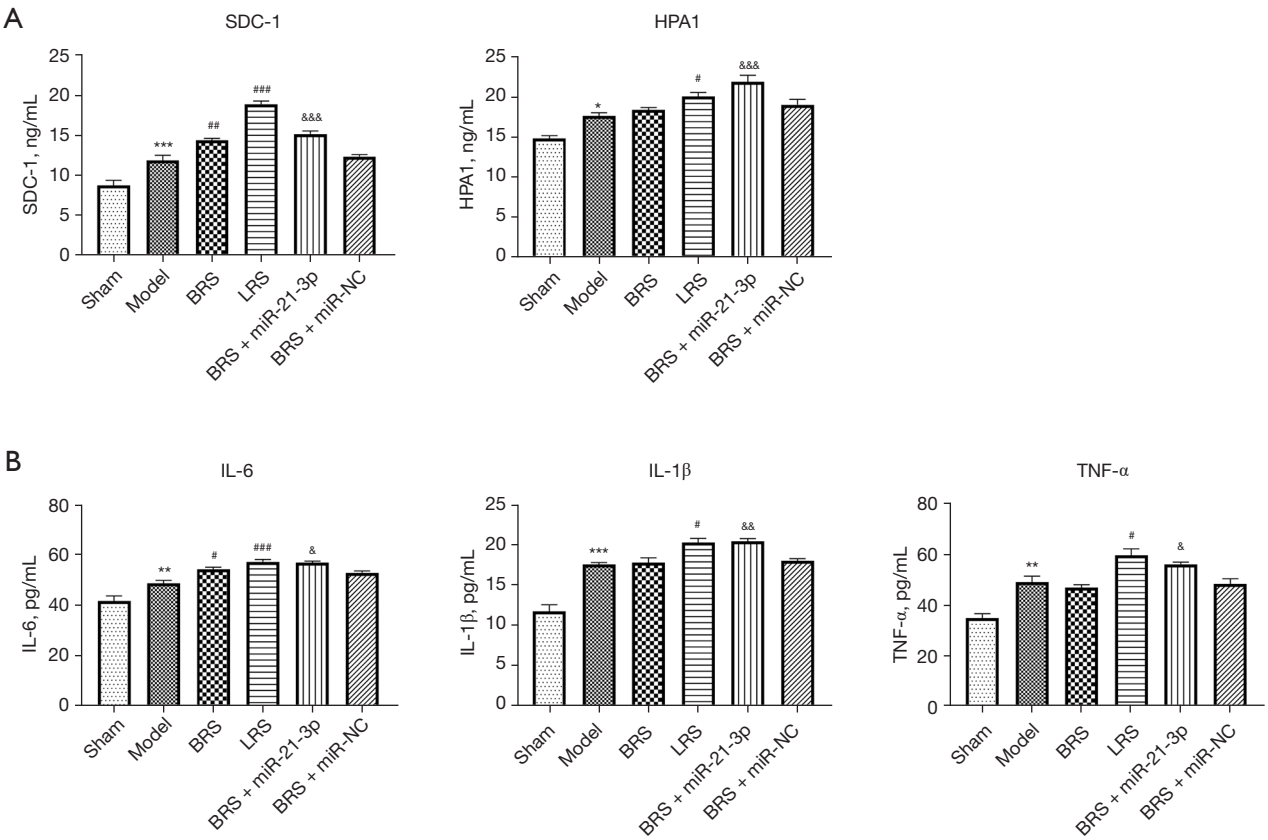

Figure 6 MiR-21-3p destroyed the glycocalyx and induced inflammation in the THS rats treated with BRS. The levels of SDC-1, HPA1 (A), and IL-6, IL-1β, and TNF-α (B) in the serum of the BRS-treated THS rats transfected with lentivirus-mediated miR-21-3p were determined by their respective ELISA kits. *, P<0.05; **, P<0.01; ***, P<0.001, *vs.* sham. #, P<0.05; ##, P<0.01; ###, P<0.001, *vs.* model. &, P<0.05; &&, P<0.01; &&&, P<0.001, *vs.* BRS + miR-NC. THS, traumatic hemorrhagic shock; BRS, bicarbonate Ringer's solution; LRS, lactate Ringer's solution; NC, negative control; SDC-1, syndecan-1; HPA1, heparanase-1; IL, interleukin; TNF-α, tumor necrosis factor α.

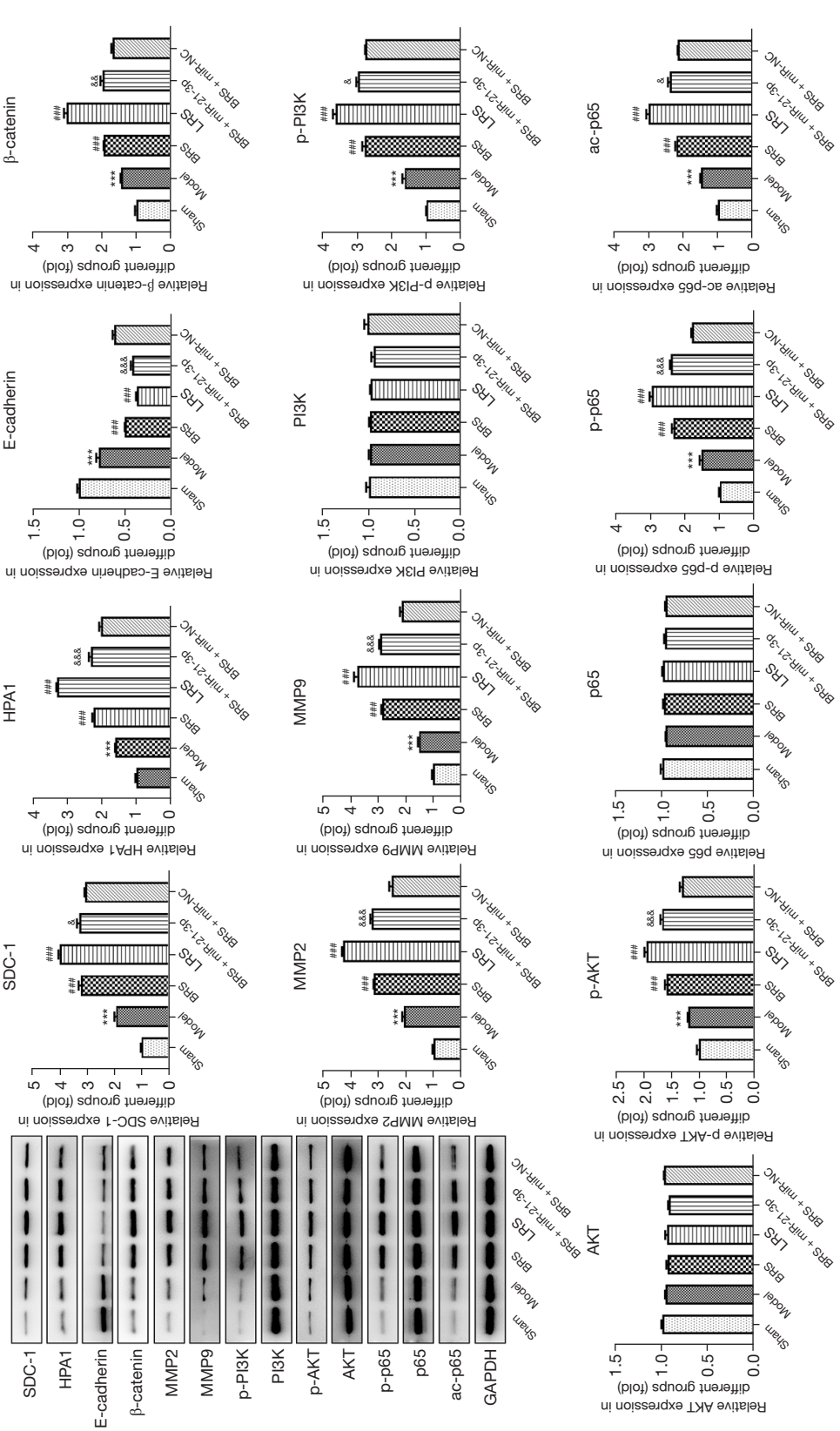

Figure 7 MiR-21-3p regulated the PI3K/Akt/NF-κB signaling pathway. The related protein expression of the glycocalyx, cell junction, and PI3K/Akt/NF-κB signaling pathway was detected by Western blot. ***, P<0.001, *vs.* sham. ###, P<0.001, *vs.* model. &, P<0.05; &&, P<0.01; &&&, P<0.001, *vs.* BRS + miR-NC. ac, acetylated; p, phosphorylated; BRS, bicarbonate Ringer's solution; LRS, lactate Ringer's solution; NC, negative control; SDC-1, syndecan-1; HPA1, heparanase-1; MMP, matrix metallopeptidase; PI3K, phosphatidylinositol 3-kinase; Akt, protein kinase B; GAPDH, glyceraldehyde 3-phosphate dehydrogenase.

functional destruction of the endodermis glycocalyx (44,45).

E-cad is an adhesive receptor, and β-catenin is a protein that interacts with the intracellular segment of E-cad. Together, the 2 form the E-cad/β -catenin complex, which is important in maintaining the integrity and polarity of epithelial cells, and β-catenin is a major regulator of the function of the whole complex (46). We found that the levels of SDC-1, HPA1, β-catenin, MMP2, and MMP9 were increased in the model group, and were further promoted by BRS or LRS, while E-cad expression was decreased in the model group, and was further downregulated in the BRS and LRS groups. Thus, our experimental results indicated that BRS had a better clinical effect than LRS on THS.

MiR-21-3p is a miRNA that mediates the inflammatory response. When pancreatitis occurs, pancreatic cells are damaged, which can promote the release of miR-21-3p, which in turn has been shown to aggravate injury in rats with acute hemorrhagic necrotizing pancreatitis (47). MiR-21-3p has also been shown to be increased in brain microvascular endothelial cells, which in turn promotes apoptosis and inflammation (25). The expression of miR-21-3p is increased by LPS induction, and the downregulation of miR-21-3p alleviates inflammatory responses and apoptosis caused by LPS in retinal pigment epithelial cells (48). In this study, we reported that the levels of pro-inflammatory factors (i.e., IL-6, IL-1β, and TNF-α) in the BRS group were enhanced by miR-21-3p transfection.

The PI3K/Akt signaling pathway is a classic intracellular signaling pathway and a key transducer for metabolism and mitogenic signaling, regulating gene expression protein translation and cell metabolism, and thus regulating cell growth and proliferation (49). Activated Akt is transferred from the cell membrane to the cytoplasm or nucleus, where it continues to target downstream signaling molecules, such as mammalian/mechanistic target of rapamycin (mTOR) and nuclear factor kappa B (NF-κB) (50). The PI3K/Akt/NF-κB signaling pathway is one of the major signaling pathways that regulate stress and fight inflammation (51,52).

NF-κB exacerbates inflammatory injury, and TNF-α induces the degradation of NF-κB inhibitor IκB, thereby enhancing NF-κB activity and promoting the synthesis and release of TNF-α, IL-1, and IL-6, forming a cascade reaction (53,54). Following hemorrhagic shock, NF-κB activates an inflammatory cascade that accelerates the release of pro-inflammatory factors, such as TNF-α (55). The inhibition of IκB kinase/NF-κB signaling by BAY11-7082 was shown to improve the proinflammatory response of microvascular endothelial cells in mice with hemorrhagic shock (56). Previous studies by our team have shown that the inhibition of NF-κB P65 protein and activation of toll like receptor 4 (TLR4)/NF-κB signaling pathway reduced pro-inflammatory cytokines (TNF-α, IL-1, and IL-6) and increased anti-inflammatory cytokines (IL-4 and IL-10) in hemorrhagic shock rats and thus reversed the imbalance of inflammatory mediators and reduced organ damage caused by THS (57,58).

PI3K/Akt/NF-κB signaling is also widely involved in the regulation of endothelial cells. For example, the apoptosis of endothelial cells was shown to be reduced by miR-126-5p through the inactivation of the NF-κB-mediated PI3K/Akt/mTOR signaling pathway (59). Myristicin suppresses the promotive effects of oxidized low-density lipoprotein (ox-LDL) on the PI3K/Akt and NF-κB signaling pathway in both human vascular smooth muscle cells (hVSMCs) and HUVECs (60). Hepatocyte growth factor promotes the motility of lung endothelial cells by activating the c-Met/PI3K/Akt signaling pathway (61).

MiR-21-3p suppresses the sensitivity of liver cancer stem cells toward TNF-related apoptosis-inducing ligand by activating the PI3K/Akt/Bad cascade (62). Previous studies have shown that the PI3K/Akt and TLR4/NF-κB signaling pathways are important targets of miR-21 (63,64). The upregulation of miR-21 has been shown to promote the expression levels of both PI3K and Akt in ox-LDL-treated VSMC, while the inhibition of miR-21 suppresses the inflammatory response of ox-LDL-treated HUVECs by inactivating the TLR4/NF-κB signaling pathway (65). MiR-21 promotes the expression of NF-κB and NLRP3 in RAW264.7 cells (66). MiR-21 was confirmed to promote NF-κB activation and thereby increase the activity of Akt, a kinase known to promote the NF-κB pathway (67). This study also indicated that miR-21-3p promoted the inflammation and glycocalyx damage of pulmonary vascular endothelial cells by activating the PI3K/Akt/NF-κB signaling pathway in the THS rats treated with BRS.

Conclusions

In summary, BRS and LRS all had a damaged effect on lung tissues while LRS had a more injurious effect on lung tissues than BRS. the expression of miR-21-3p was increased in the THS rats resuscitated with BRS or LRS. Among the groups, miR-21-3p expression was higher in the THS rats resuscitated with LRS. Further, miR-21-3p promoted inflammation and glycocalyx damage by

activating the PI3K/Akt/NF-κB signaling pathway, thereby aggravating the lung injury in the THS rats resuscitated with BRS. This study had some limitations. Notably, it only investigated the effect of miR-21-3p on lung injury in the THS rats resuscitated with BRS, and other organ injuries need to be explored. In addition, the inhibitor or agonist of signaling pathway were not used to confirm the role of PI3K/Akt/NF-κB signaling pathway in THS. The problems and challenges are existed in clinical application of miRNA. First, the identified and characterized miRNA markers need to be independently validated with large sample sizes. Second, change in clinical practice guidelines encounter considerable resistance because this requires extensive education and expertise to accept new diagnostic or prognostic tools across physicians, administrators, and laboratory personnel.

Acknowledgments

Funding: This study was supported by the Key Laboratory of Emergency and Trauma (Hainan Medical University), Ministry of Education Grant (No. KLET-202106).

Footnote

Reporting Checklist: The authors have completed the ARRIVE reporting checklist. Available at https://atm.amegroups.com/article/view/10.21037/atm-22-5148/rc

Data Sharing Statement: Available at https://atm.amegroups.com/article/view/10.21037/atm-22-5148/dss

Conflicts of Interest: All authors have completed the ICMJE uniform disclosure form (available at https://atm.amegroups.com/article/view/10.21037/atm-22-5148/coif). The authors have no conflicts of interest to declare.

Ethical Statement: The authors are accountable for all aspects of the work in ensuring that questions related to the accuracy or integrity of any part of the work are appropriately investigated and resolved. Animal experiments were performed under a project license (No. 2022101) granted by the Animal Care and Use Committee and the Animal Ethics Committee of The First Affiliated Hospital of Bengbu Medical College, in compliance with national guidelines for the care and use of animals.

References

1. Cannon JW. Hemorrhagic Shock. N Engl J Med 2018;378:370-9.
2. Divo MJ, Martinez CH, Mannino DM. Ageing and the epidemiology of multimorbidity. Eur Respir J 2014;44:1055-68.
3. Lozano R, Naghavi M, Foreman K, et al. Global and regional mortality from 235 causes of death for 20 age groups in 1990 and 2010: a systematic analysis for the Global Burden of Disease Study 2010. Lancet 2012;380:2095-128.
4. Eastridge BJ, Holcomb JB, Shackelford S. Outcomes of traumatic hemorrhagic shock and the epidemiology of preventable death from injury. Transfusion 2019;59:1423-8.
5. Weber B, Mendler MR, Lackner I, et al. Lung injury after asphyxia and hemorrhagic shock in newborn piglets: Analysis of structural and inflammatory changes. PLoS One 2019;14:e0219211.
6. Fox EE, Holcomb JB, Wade CE, et al. Earlier Endpoints are Required for Hemorrhagic Shock Trials Among Severely Injured Patients. Shock 2017;47:567-73.
7. Jiang JK, Fang W, Hong LJ, et al. Distribution and differentiation of myeloid-derived suppressor cells after fluid resuscitation in mice with hemorrhagic shock. J Zhejiang Univ Sci B 2017;18:48-58.
8. Jiang LM, He J, Xi XY, et al. Effect of early restrictive fluid resuscitation on inflammatory and immune factors in patients with severe pelvic fracture. Chin J Traumatol 2019;22:311-5.
9. Gazmuri RJ, Whitehouse K, Whittinghill K, et al. Early and sustained vasopressin infusion augments the hemodynamic efficacy of restrictive fluid resuscitation and improves survival in a liver laceration model of hemorrhagic shock. J Trauma Acute Care Surg 2017;82:317-27.
10. Li Q, Zhu H, Qiu Z, et al. Effects of different fluid-restricted resuscitation on the expression of Th17,

Treg cells and related cytokines in peripheral blood of patients with traumatic hemorrhagic shock and its clinical significance. Journal of Bengbu Medical College 2020;45:291-5.
11. Zhao X, Zhu J, Zhang X. Effects of restricted fluid resuscitation on inflammatory injury and multisystem organ function in patients with traumatic shock. Laboratory Medicine and Clinic 2021;18:2087-90.
12. Liu G. Fluid resuscitation strategy for traumatic hemorrhagic shock. Chinese Journal of Emergency Medicine 2018,27:473-5.
13. Zhao D, Zhang F, Xu Z, et al: Effect of limited resuscitation with sodium bicarbonate Ringer's solution on the internal environment of traumatic hemorrhagic shock. Journal of Bengbu Medical College 2021;46:447-50.
14. Wang L, Lou J, Cao J, et al. Bicarbonate Ringer's solution for early resuscitation in hemorrhagic shock rabbits. Ann Transl Med 2021;9:462.
15. Shires GT, Browder LK, Steljes TP, et al. The effect of shock resuscitation fluids on apoptosis. Am J Surg 2005;189:85-91.
16. Ma J, Han S, Liu X, et al. Sodium bicarbonated Ringer's solution effectively improves coagulation function and lactic acid metabolism in patients with severe multiple injuries and traumatic shock. Am J Transl Res 2021;13:5043-50.
17. Satoh K, Ohtawa M, Katoh M, et al. Pharmacological study of BRS, a new bicarbonated Ringer's solution, in haemorrhagic shock dogs. Eur J Anaesthesiol 2005;22:703-11.
18. Satoh K, Ohtawa M, Okamura E, et al. Pharmacological study of BRS, a new bicarbonated Ringer's solution, in partially hepatectomized rabbits. Eur J Anaesthesiol 2005;22:624-9.
19. Nelson A, Statkevicius S, Schött U, et al. Effects of fresh frozen plasma, Ringer's acetate and albumin on plasma volume and on circulating glycocalyx components following haemorrhagic shock in rats. Intensive Care Med Exp 2016;4:6.
20. Lipowsky HH. Role of the Glycocalyx as a Barrier to Leukocyte-Endothelium Adhesion. Adv Exp Med Biol 2018;1097:51-68.
21. Cao RN, Tang L, Xia ZY, et al. Endothelial glycocalyx as a potential theriapeutic target in organ injuries. Chin Med J (Engl) 2019;132:963-75.
22. Smart L, Boyd CJ, Claus MA, et al. Large-Volume Crystalloid Fluid Is Associated with Increased Hyaluronan Shedding and Inflammation in a Canine Hemorrhagic Shock Model. Inflammation 2018;41:1515-23.
23. Zhang X, Sun D, Song JW, et al. Endothelial cell dysfunction and glycocalyx - A vicious circle. Matrix Biol 2018;71-72:421-31.
24. Saliminejad K, Khorram Khorshid HR, Soleymani Fard S, et al. An overview of microRNAs: Biology, functions, therapeutics, and analysis methods. J Cell Physiol 2019;234:5451-65.
25. Ge X, Li W, Huang S, et al. Increased miR-21-3p in Injured Brain Microvascular Endothelial Cells after Traumatic Brain Injury Aggravates Blood-Brain Barrier Damage by Promoting Cellular Apoptosis and Inflammation through Targeting MAT2B. J Neurotrauma 2019;36:1291-305.
26. Jiang Y, Xie H, Tu W, et al. Exosomes secreted by HUVECs attenuate hypoxia/reoxygenation-induced apoptosis in neural cells by suppressing miR-21-3p. Am J Transl Res 2018;10:3529-41.
27. Shao M, Yu M, Zhao J, et al. miR-21-3p regulates AGE/RAGE signalling and improves diabetic atherosclerosis. Cell Biochem Funct 2020;38:965-75.
28. Livak KJ, Schmittgen TD. Analysis of relative gene expression data using real-time quantitative PCR and the 2(-Delta Delta C(T)) Method. Methods 2001;25:402-8.
29. Chen C, Li Q, Jiang H. Research progress on treatment strategy of acute lung injury after traumatic hemorrhagic shock. Shanghai Medical Journal 2014;37:162-5.
30. Vernon PJ, Paredes RM, Sooter AJ, et al. Severe Hemorrhagic Shock Induces Acute Activation and Expansion of IL-8+/IL-10+ Neutrophils with Enhanced Oxidative Reactivity in Non-Human Primates. Shock 2016;46:129-36.
31. Batistaki C, Kostopanagiotou G, Myrianthefs P, et al. Effect of exogenous catecholamines on tumor necrosis factor alpha, interleukin-6, interleukin-10 and beta-endorphin levels following severe trauma. Vascul Pharmacol 2008;48:85-91.
32. Kusza K, Mielniczuk M, Krokowicz L, et al. Ringer's lactate solution enhances the inflammatory response during fluid resuscitation of experimentally induced haemorrhagic shock in rats. Arch Med Sci 2018;14:655-70.
33. Chepurnova DA, Samoilova EV, Anisimov AA, et al. Compounds of IL-6 Receptor Complex during Acute Lung Injury. Bull Exp Biol Med 2018;164:609-11.
34. Buckland J. Experimental arthritis: Fire and ice: syndecan-3 in inflammation. Nat Rev Rheumatol 2014;10:514.
35. Wu F, Peng Z, Park PW, et al. Loss of Syndecan-1

Abrogates the Pulmonary Protective Phenotype Induced by Plasma After Hemorrhagic Shock. Shock 2017;48:340-5.
36. Jackson-Weaver O, Friedman JK, Rodriguez LA, et al. Hypoxia/reoxygenation decreases endothelial glycocalyx via reactive oxygen species and calcium signaling in a cellular model for shock. J Trauma Acute Care Surg 2019;87:1070-6.
37. Wiesinger A, Peters W, Chappell D, et al. Nanomechanics of the endothelial glycocalyx in experimental sepsis. PLoS One 2013;8:e80905.
38. Kang H, Liu J, Yu M, et al. The development of the visualization and measurement techniques of the endothelial glycocalyx. Chinese Bulletin of Life Sciences 2016,28:1089-99.
39. Jiang T. Protective effect of heparin on endothelial glycocalyx during sepsis in rat model. Nanjing: Southeast University, 2014.
40. Duan CY, Zhang J, Wu HL, et al. Regulatory mechanisms, prophylaxis and treatment of vascular leakage following severe trauma and shock. Mil Med Res 2017;4:11.
41. Vestweber D. VE-cadherin: the major endothelial adhesion molecule controlling cellular junctions and blood vessel formation. Arterioscler Thromb Vasc Biol 2008;28:223-32.
42. Bauer AT, Bürgers HF, Rabie T, et al. Matrix metalloproteinase-9 mediates hypoxia-induced vascular leakage in the brain via tight junction rearrangement. J Cereb Blood Flow Metab 2010;30:837-48.
43. Higashida T, Kreipke CW, Rafols JA, et al. The role of hypoxia-inducible factor-1α, aquaporin-4, and matrix metalloproteinase-9 in blood-brain barrier disruption and brain edema after traumatic brain injury. J Neurosurg 2011;114:92-101.
44. Gronski TJ Jr, Martin RL, Kobayashi DK, et al. Hydrolysis of a broad spectrum of extracellular matrix proteins by human macrophage elastase. J Biol Chem 1997;272:12189-94.
45. Kuehn R, Kaczensky P, Lkhagvasuren D, et al. Differentiation of Meat Samples from Domestic Horses (Equus caballus) and Asiatic Wild Asses (Equus hemionus) Using a Species-Specific Restriction Site in the Mitochondrial Cytochrome b Region. Mong J Biol Sci 2006;4:57-62.
46. Harrington KJ, Syrigos KN. The role of E-cadherin-catenin complex: more than an intercellular glue? Ann Surg Oncol 2000;7:783-8.
47. Wang T, Jiang L, Wei X, et al. MiR-21-3p aggravates injury in rats with acute hemorrhagic necrotizing pancreatitis by activating TRP signaling pathway. Biomed Pharmacother 2018;107:1744-53.
48. Liu J, Ma Z, Ran Z. MiR-21-3p modulates lipopolysaccharide-induced inflammation and apoptosis via targeting TGS4 in retinal pigment epithelial cells. Clin Exp Pharmacol Physiol 2019;46:883-9.
49. Very N, Vercoutter-Edouart AS, Lefebvre T, et al. Cross-Dysregulation of O-GlcNAcylation and PI3K/AKT/mTOR Axis in Human Chronic Diseases. Front Endocrinol (Lausanne) 2018;9:602.
50. Zhang G, Wang Q, Wang W, et al. Tempol Protects Against Acute Renal Injury by Regulating PI3K/Akt/mTOR and GSK3β Signaling Cascades and Afferent Arteriolar Activity. Kidney Blood Press Res 2018;43:904-13.
51. Pan T, Shi X, Chen H, et al. Geniposide Suppresses Interleukin-1β-Induced Inflammation and Apoptosis in Rat Chondrocytes via the PI3K/Akt/NF-κB Signaling Pathway. Inflammation 2018;41:390-9.
52. Lou Y, Wang C, Tang Q, et al. Paeonol Inhibits IL-1β-Induced Inflammation via PI3K/Akt/NF-κB Pathways: In Vivo and Vitro Studies. Inflammation 2017;40:1698-706.
53. Zhang YF, Zou XL, Wu J, et al. Rosiglitazone, a Peroxisome Proliferator-Activated Receptor (PPAR)-γ Agonist, Attenuates Inflammation Via NF-κB Inhibition in Lipopolysaccharide-Induced Peritonitis. Inflammation 2015;38:2105-15.
54. Belinga VF, Wu GJ, Yan FL, et al. Splenectomy following MCAO inhibits the TLR4-NF-κB signaling pathway and protects the brain from neurodegeneration in rats. J Neuroimmunol 2016;293:105-13.
55. El-Tahan RR, Ghoneim AM, El-Mashad N. TNF-α gene polymorphisms and expression. Springerplus 2016;5:1508.
56. Li R, Aslan A, Yan R, et al. Histone Deacetylase Inhibition and IκB Kinase/Nuclear Factor-κB Blockade Ameliorate Microvascular Proinflammatory Responses Associated With Hemorrhagic Shock/Resuscitation in Mice. Crit Care Med 2015;43:e567-80.
57. Xu ZP, Song Q, Qiu ZL, et al. The effect of acetate Ringer's solution on inflammatory factors and NF-κB signal pathway in the liver of hemorrhagic shock rats. Genetics and Molecular Research 2018;17:gmr16039906.
58. Chen Y, Xu Z, Song Q, et al. Mechanism of ulinastatin in reducing lung inflammatory injury in rats with hemorrhagic shock. Journal of Southern Medical University 2019;39:1232-8.
59. Jia W, Liu J, Tian X, et al. MircoRNA-126-5p inhibits apoptosis of endothelial cell in vascular arterial walls

via NF-κB/PI3K/AKT/mTOR signaling pathway in atherosclerosis. J Mol Histol 2022;53:51-62.
60. Luo L, Liang H, Liu L. Myristicin regulates proliferation and apoptosis in oxidized low-density lipoprotein-stimulated human vascular smooth muscle cells and human umbilical vein endothelial cells by regulating the PI3K/Akt/NF-κB signalling pathway. Pharm Biol 2022;60:56-64.
61. Usatyuk PV, Fu P, Mohan V, et al. Role of c-Met/phosphatidylinositol 3-kinase (PI3k)/Akt signaling in hepatocyte growth factor (HGF)-mediated lamellipodia formation, reactive oxygen species (ROS) generation, and motility of lung endothelial cells. J Biol Chem 2014;289:13476-91.
62. Zhu Y, Tang H, Zhang L, et al. Suppression of miR-21-3p enhances TRAIL-mediated apoptosis in liver cancer stem cells by suppressing the PI3K/Akt/Bad cascade via regulating PTEN. Cancer Manag Res 2019;11:955-68.
63. Lin F, Yin HB, Li XY, et al. Bladder cancer cell-secreted exosomal miR-21 activates the PI3K/AKT pathway in macrophages to promote cancer progression. Int J Oncol 2020;56:151-64.
64. Pan YQ, Li J, Li XW, et al. Effect of miR-21/TLR4/NF-κB pathway on myocardial apoptosis in rats with myocardial ischemia-reperfusion. Eur Rev Med Pharmacol Sci 2018;22:7928-37.
65. Pei X, Wen Y, Cui F, et al. lncRNA CASC7 regulates pathological progression of ox-LDL-stimulated atherosclerotic cell models via sponging miR-21 and regulating PI3K/Akt and TLR4/NF-κB signaling pathways. Aging (Albany NY) 2021;13:25408-25.
66. Zhao B, Shi Z, Zhang S, et al. miR-21 promotes expression of NF-κB and NLRP3 in mouse RAW264.7 cells by inhibiting A20. Xi Bao Yu Fen Zi Mian Yi Xue Za Zhi 2021;37:140-5.
67. Choudhury SN, Li Y. miR-21 and let-7 in the Ras and NF-κB pathways. Microrna 2012;1:65-9.

(English Language Editor: L. Huleatt)

Cite this article as: Xu S, Qiu Z, Zheng C, Li L, Jiang H, Zhang F, Wang Z. Effect of miR-21-3p on lung injury in rats with traumatic hemorrhagic shock resuscitated with sodium bicarbonate Ringer's solution. Ann Transl Med 2022;10(24):1331. doi: 10.21037/atm-22-5148

